Isothermal P, x, y Data for the Nitrogen + Carbon Monoxide System at five Temperatures from 100 to 130 K and Pressures up to 3.4 MPa

Xavier Courtial, Alain Valtz, Salaheddine Chabab, Christophe Coquelet, Philippe Arpentinier

Isothermal *P*, *x*, *y* Data for the Nitrogen + Carbon Monoxide System at five Temperatures from 100 to 130 K and Pressures up to 3.4 MPa

Xavier Courtial[a+], Alain Valtz[a], Salaheddine Chabab[a,d],

Christophe Coquelet[a,c*], Philippe Arpentinier[a,b*]

[a] Mines ParisTech, PSL University, CTP- Centre of Thermodynamics of Processes, 77305 Fontainebleau, France.
[b] Air Liquide Innovation Campus Paris, 1, chemin de la porte des Loges, Les Loges en Josas 78354 Jouy en Josas Cedex
[c] : Université de Toulouse, Mines Albi, Centre RAPSODEE UMR CNRS 5302, Campus Jarlard, Albi, France
[d] : Univ Pau & Pays Adour, Laboratoire de Thermique, Energetique et Procédés (LaTEP), Rue Jules Ferry BP 7511, 64075 Pau Cedex, France

---

Isothermal vapor-liquid equilibrium (VLE) data have been measured for the nitrogen + carbon monoxide binary system at 5 temperatures from 100.01 to 130.07 K, and at pressures from 0.37 to 3.35 MPa. This system had already been studied by different authors. Nevertheless, the existing literature data generally indicate high vapor pressure for pure CO and for the highest CO composition in the N_2-CO binary VLE measurements. Our new VLE data have been measured using the "static-analytic" method, taking advantage of two pneumatic capillary samplers (Rolsi®, Armines' patent) coupled to an adapted apparatus able to work at cryogenic temperatures. The new data were compared with the predictions of the GERG equation of state and their consistency was checked by a Van Ness type test. We have observed that the isothermal *P*, *x*, *y* data were well represented with the Peng-Robinson equation of state, especially in the CO rich region.

Keywords: Cryogeny, experimental work, vapor liquid equilibrium, data treatment, Helmholtz energy model, Peng Robinson Equation of State.

---

*: Corresponding authors:
E-mail: christophe.coquelet@mines-albi.fr Phone (33) 5634931341
E-mail: philippe.arpentinier@airliquide.com Phone: (33) 1629749071.

+ current adress : AXENS, Avenue Jean Moulin CS 30319, 30340 Salindres – France

1. Introduction

The production of a syngas rich in carbon monoxide (CO) and hydrogen (H_2) from methane (CH_4) is an important step in the valorization of natural gas. The two main industrial processes currently in use are steam methane reforming and partial oxidation of methane. Carbon monoxide is used in the chemical industry for the synthesis of many compounds: methanol, acetic, formic and acrylic acids, aldehydes, phosgene, etc. It is also used in metallurgy as a reducing agent and for the regeneration of catalysts. Another application of carbon monoxide is the Fischer-Tropsch conversion of syngas into liquid fuels, which is currently being exploited in countries with inexpensive carbon sources (South Africa, Malaysia, and Qatar).

Pure carbon monoxide can be produced from syngas after separation and purification. These operations can be conducted industrially by two types of processes which are carried out by industrial gas companies: partial condensation of syngas components and scrubbing of syngas by liquefied gases, particularly methane.

Historically, partial condensation is the first cryogenic separation of syngas; the separation is based on the difference of boiling temperatures of the compounds contained in the syngas. In principle, this treatment, which applies to syngas available under pressure and previously dried and decarbonized, comprises the following operating steps: cooling of the feedstock by heat exchange with the products, partial condensation of some of the components, liquid/vapor separation. Partial condensation is usually implemented to supply pure CO with a recovery comprised between 85 and 95%. Relatively pure hydrogen (98 mol.%) at low pressure is also produced with a recovery of about 97%.

Scrubbing of syngas by liquid methane is another option: the available syngas, previously dried and decarbonized, is cooled in countercurrent flow by the cold purified products, and is then introduced at the bottom of a column with a down flow of liquid

methane. This operation yields hydrogen with a purity better than 98.5 mol.% and containing less than 10 ppm of carbon monoxide. After expansion and partial vaporization, the extract feeds a column operating at low pressure (2 bar) which separates carbon monoxide at the top at a purity over 99 mol.%, and liquid methane at the bottom which is recycled to the scrubbing column. Methane scrubbing is usually implemented to supply pure carbon monoxide with a recovery of about 99%. Relatively pure hydrogen (98.5 mol.%) is also produced with a recovery of about 97%.

When the nitrogen content of the natural gas used as feed to produce hydrogen is high and/or when the carbon monoxide specification fixed by its downstream use assesses very low nitrogen content, a nitrogen removal column is required. This low-pressure column can be added both on partial condensation and methane scrubbing processes. Due to the proximity of nitrogen and carbon monoxide in terms of vapor pressure, this unit operation is energy consuming and thus, cold and heat required respectively in the condenser and in the reboiler of the column can be supplied by a nitrogen or a carbon monoxide cold cycle. Due to the low relative volatility of this binary system (K_{N2}/K_{CO} ~1.2 at 116 K), it should be noted that the thermodynamic model used for designing such a column should be as accurate as possible to avoid an over or underestimation of its number of theoretical trays.

Another area interested in the knowledge of liquid/vapor equilibrium data of the N_2-CO is the CO_2 capture transport and storage (CCS). Technologies involved in this field have to separate CO_2 from water, SOx, NOx and air gases. They require accurate thermodynamic model as the ideal gas thermodynamic property model differ strongly from the real fluid properties. The development of such thermodynamic model to design CCS process requires binary interaction parameters (Coquelet et al. [1]). Indeed, cryogenic compounds like NO, CO, N_2 and Ar are also impurities present within CO_2

after the process of CO_2 capture. The partnership between the Centre de Thermodynamique des Procédés (CTP) and Air Liquide R&D has already led to the publication of experimental data of binary system composed with CO_2 and such impurities (CO_2-Ar (Coquelet et al. [2], CO_2-SO_2, CO_2-NO (Coquelet et al. [3]). Also, binary interaction parameters (BIPs) concerning each binary system involving two impurities are required. For example, in 2018, Zhang et al. [4] have published new experimental data and have adjusted BIPs for the binaries (NO-CO, NO-N_2 and NO-Ar) presented in the CO_2-rich mixture. This work will complete the data set of system of interest in the context of CO_2 transportation and underground storage.

The N_2 + CO binary system is type I according to the classification of van Konynenburg and Scott [5] as a consequence of a mixture of normal fluids (simple molecules), presenting a simple behaviour.

In 2016, Gernet and Span [6] have published an equation of state based on Helmholtz energy for CO_2 rich mixtures typical for CCS application. The model was developed considering PρT data, VLE data and second virial coefficient data of the N_2 + CO binary system. Concerning the experimental VLE data available, we can cite the data published by Sprow and Prausnitz [7] at 83.82 K, by Torocheshnikov [8] between 70 and 122 K, by Yushkevich and Torochechnikov [9] between 70 and 121.80 K, Pool et al. [10] at 83.82 K and Duncan et al. [11] at 68.09 K. Even if there are many data sets, especially from Torocheshnikov and Yushkevich and Torochechnikov, there is no data which describe very well the highest CO molar fraction. This point was also mention by Gernet and Span (lowest molar fraction of N_2 identify 0.11). Moreover, to the knowledge of the authors, there is no data for temperature higher than the critical temperature of nitrogen.

In this paper, new VLE data are presented concerning the N_2+ CO binary system at 5 temperatures between 100.02 and 130.07 K. Our new data intend to describe particularly the part for low nitrogen molar fraction.

The experimental results are fitted using the Peng-Robinson Equation of State (PR EoS). The pure component *PT* lines are also presented together with the mixture critical line calculated using the parameters adjusted on our binary VLE data.

2. Experimental Section.

2.1. Materials

The two fluids were obtained from Air Liquide with a certified purity higher than 99.997 vol % for the CO and 99.995 vol % for the Nitrogen (Table 1). No further purification was performed before use.

Table 1: Chemicals sample

Chemical Name	CAS number	Source	Initial Vol.% Purity	Purification Method	Final Mole Fraction Purity	Analysis Method
Carbon monoxide	7727-37-9	Air Liquide	99.997	none	-	SM[a]
Nitrogen	630-8-0	Air Liquide	99.995	none	-	SM

a Supplier Method

2.2. Apparatus

The apparatus used in this work is based on a “static-analytic” method with sampling of the liquid and vapor phase. It is similar to that described by Houssin et al.

[12]. The internal volume of the equilibrium cell is around 43 cm^3. For accurate thermal regulation, it is introduced in a brass block with a heater regulated by a PID regulator (WEST, model 6100) monitoring its temperature. To obtain low temperatures, liquid nitrogen is introduced into a 55 liter Dewar and the cell is immersed in the nitrogen vapor space at about the nitrogen boiling temperature (77.34 K [13]). Pressures are measured using two pressure transducers (Druck, type PTX611, range: 0 – 1 and 0 – 16 MPa). These sensors are calibrated against a dead weight pressure balance (5202S model from Desgranges & Huot, CP 0.3 to 40 MPa, Aubervilliers, France).

Temperatures are measured with two Pt100 platinum resistance thermometer probes inside the walls of the equilibrium cell. The two Pt100 thermo probes were calibrated through pressure comparisons between measured vapor pressures of pure oxygen (99.995 vol % purity) and calculated vapor pressures from DIPPR correlation [13] for this component. The pure component is loaded inside the cell and kept at constant temperature. Accurate vapor pressures of the pure component are measured by the previously calibrated pressure transducer. Thereafter through DIPPR correlation [13] presenting vapor pressure of oxygen versus temperature, the platinum probes can be calibrated. A second order polynomial expression is used for representing the temperature. Pressure and temperature data acquisitions are performed with a computer linked to an Agilent unit (HP34970A). The estimated uncertainties of the transducers are u(T, k=2)=0.03 K for temperatures from 80 to 150 K, u(P, k=2)=0.00015 MPa for pressures lower than 1.5 MPa and u(P, k=2)=0.0004 MPa for pressures higher than 1.5 MPa as a result of careful calibrations.

The analytical work has been carried out using a gas chromatograph (Perichrom model PR 2100) equipped with a thermal conductivity detector (TCD) connected to a data acquisition system (Winilab III, ver. 4.0, from Perichrom). A 5 Å Molecular Sieve semi-

capillary column (0.53 mm, 25 m length, from Resteck France) kept at 313 K with a 14 mL.min^{-1} Helium flow rate allow to separate N_2 from CO. The TCD has been calibrated by two ways depending on the nitrogen composition:

- For nitrogen molar fraction higher than 0.18, the TCD response factors for each component have been determined by introducing known amounts of each pure compound, through a 500 µL chromatographic syringe, in the injector of the gas chromatograph. Considering the uncertainties due to calibrations and dispersions of analyses, resulting uncertainties on vapor and liquid mole numbers are estimated to be less than ± 1.0 % and ± 0.7 % for N_2 and CO respectively. The resulting uncertainty on the nitrogen composition is less than u(z)= 0.0035.

- For nitrogen content lower than 0.18, the TCD response factors ratio between N_2 and CO has been determined from analyzes of several mixtures with different nitrogen content, as described in the book of Raal and Mühlbauer [14]. The mixtures have been synthesized directly inside the equilibrium cell. Compositions have been determined by introducing different quantities of each pure compound through a 13 cm^3 reservoir connected to a 4 MPa pressure transducer (with an accuracy of ± 0.0004 MPa), allowing to determine the quantities transferred inside the equilibrium cell. Dedicated expressions from ALLPROPS [15] software has been used to represent the volumetric properties of each component. In these conditions, the mixture composition is determined with uncertainty lower than u(z)=0.003 for nine mixtures of nitrogen composition from 0.009 to 0.18. A polynomial expression passing through origin is used to correlate the compositions ratio (z_1/z_2) to the chromatographic peaks areas ratio (A_1/A_2) considering that $\frac{z_1}{z_2} = l_{12}\frac{A_1}{A_2}$ (l_{12} is the response factors ratio). The resulting uncertainty is less than u(z)=0.0018.

2.3. Experimental Procedure

At room temperature, the equilibrium cell and its loading lines are evacuated until 0.1 kPa using a rotary vane vacuum pump (LEYBOLD, TRIVAC D 2.5 E model). Thereafter the temperature of the cell is decreased until the target temperature is reached, and first loaded with liquid CO (about 2 cm^3). The equilibrium temperature is assumed to be reached when the two Pt100 probes (one located at top of equilibrium cell, the other at the bottom) give equivalent temperature values within the experimental uncertainty for at least 20 minutes. After recording the vapor pressure of the CO (the heavier component) at the equilibrium temperature, the two-phase envelopes are determined with generally much more than ten *P*, *x*, *y* data. For these purposes, nitrogen (the lighter component) is introduced step by step, leading to successive equilibrium mixtures of increasing overall N_2 content. After each new N_2 loading, equilibrium is assumed when the total pressure remains unchanged within ± 1.0 kPa during a period of 20 min under efficient stirring.

For each equilibrium condition, several samples of both vapor and liquid phases are withdrawn using the pneumatic ROLSI® samplers [16] and analyzed in order to check for measurements repeatability (deviations are much less than 0.5 %).

3. Correlations

The critical temperatures (T_C), critical pressures (P_C), and acentric factors (ω), for each of the two components are provided in the Table 2.

Table 2: Pure component critical parameters from Simulis Thermodynamics software.

Compound	T_C /K	P_C/ MPa	Acentric factor
N_2	126.2	3.4000	0.0377215
CO	132.92	3.49899	0.0481621

As this binary system is classified as type I, our experimental VLE data are correlated considering a simple cubic equation of state. The Simulis Thermodynamics software (ProSim, France) is used. The Peng Robinson cubic EoS [17] is considered (Eq. 1).

$$P = \frac{RT}{v-b} - \frac{a}{v(v+b)+b(v-b)} \quad (1)$$

With $a = a_C \alpha(T_R, \omega)$; and $a_{Ci} = 0.45724 \frac{R^2 T_{Ci}^2}{P_{Ci}}$, $b_i = 0.07780 \frac{RT_{Ci}}{P_{Ci}}$, and the PPR78's alpha function (Eq. (2)).

$$\alpha_i(T_R, \omega) = \left[1 + \left(0{,}374640 + 1{,}542260\,\omega_i - 0{,}26992\,\omega_i^2\right)\left(1 - T_{Ri}^{1/2}\right)\right]^2 \quad (2)$$

The quadratic mixing rule is also considered (Eq. 3).

$$a = \sum_i \sum_j z_i z_j a_{ij} \text{ , with } a_{ij} = \sqrt{a_i a_j}\left(1 - k_{ij}\right) \text{ and } b = \sum_i z_i b_i \quad (3)$$

The binary interaction parameter (k_{ij}) value is adjusted to the VLE data using an objective function based on both bubble and dew point pressures (Eq. (4).

$$F = \frac{100}{N} \sum_1^N \left[\left(\frac{P_{BUBBLE\,cal} - P_{\exp}}{P_{\exp}} \right)^2 + \left(\frac{y_{cal} - y_{\exp}}{y_{\exp}} \right)^2 + \left(\frac{P_{DEW\,cal} - P_{\exp}}{P_{\exp}} \right)^2 + \left(\frac{x_{cal} - x_{\exp}}{x_{\exp}} \right)^2 \right] \quad (4)$$

where N is the number of data points, x_{exp} and x_{cal} are respectively the measured and calculated liquid phase mole fractions, y_{exp} and y_{cal} are respectively the measured and calculated vapor phase mole fractions, P_{exp}, $P_{BUBBLE\ cal}$ and $P_{DEW\ cal}$ are respectively the measured pressures and the bubble and dew calculated pressures.

4. Results and discussion:

4.1. Evaluation of the new measurements

The new experimental and calculated VLE data are reported in the Table 3 and plotted in the Figure 1. The results for each isotherm are presented in supplementary information as Figures S1 to S5. All data reported here passed the consistency test (Van Ness type), more details regarding the consistency test results are available in the Supplementary Material. Additional data measured at 95K that failed the test are given in the supplementary material. We have plotted the variation of relative volatility as a function of the liquid composition in figures 2a and 2b. The results are presented in more detail in figures S6 and S7 in supplementary information file.

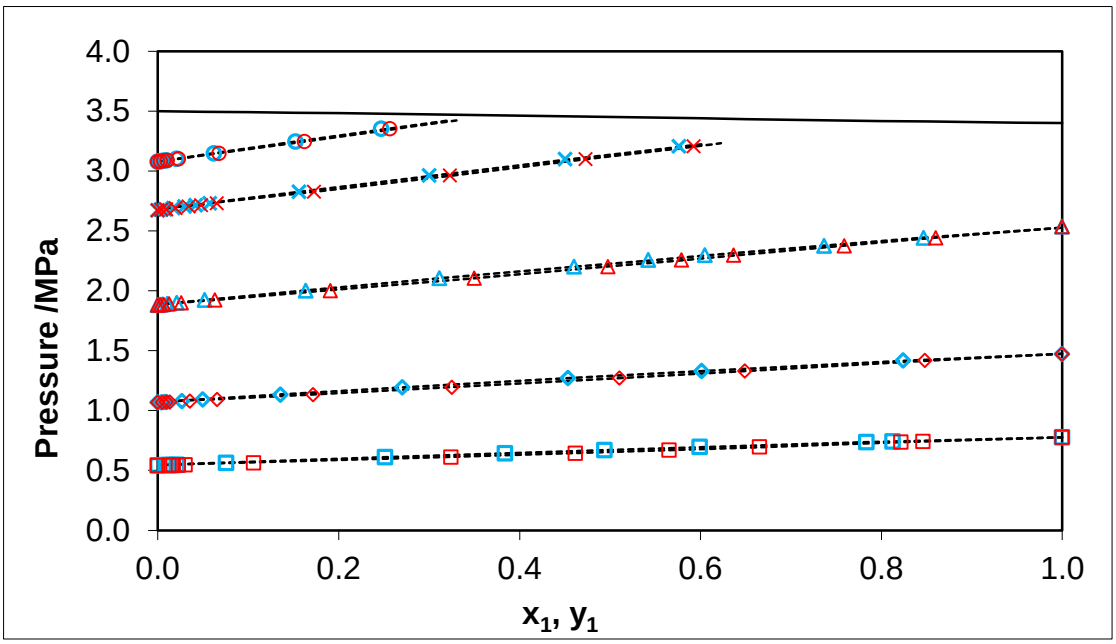

Figure 1: Phase boundaries of the binary system nitrogen (1) + carbon monoxide (2) at 100.2 (□), 110.07 (◊), 120.05 (Δ), 127.07 (×) and 130.07 K (o), experimental and calculated values (symbols this work (in blue: bubble point, in red: dew point), dashed line: PR EoS, solid line: mixture critical line).

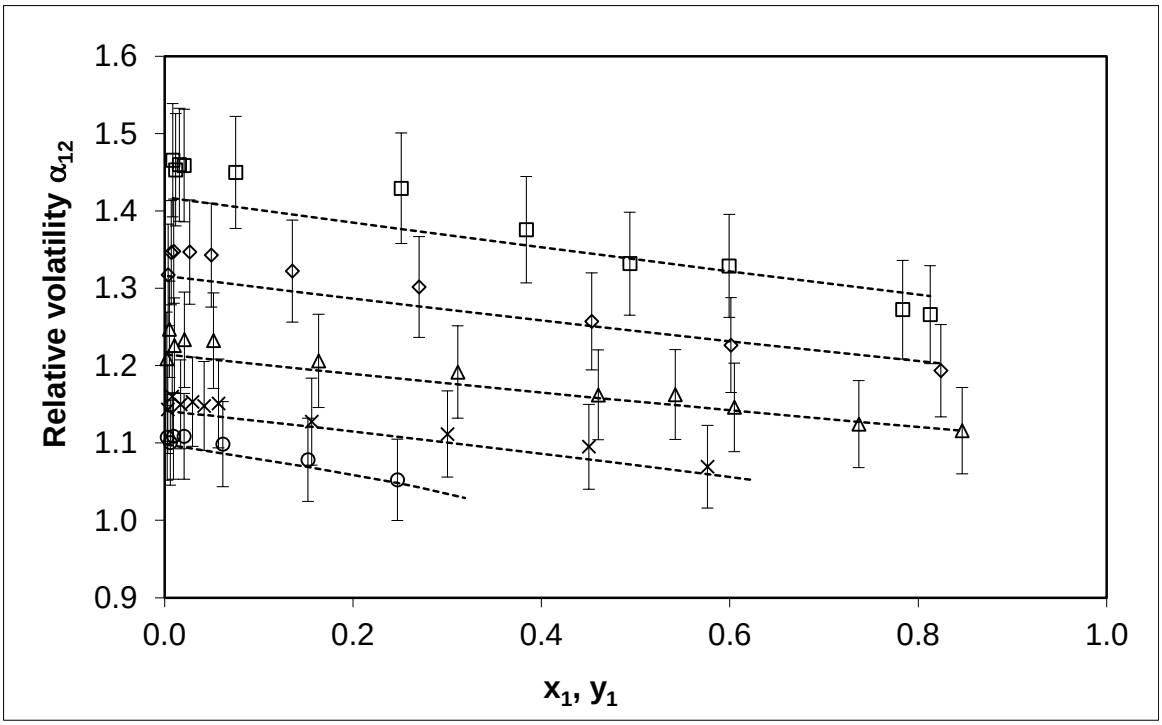

Figure 2a: Variation of the relative volatility α_{12} of the nitrogen (1) + carbon monoxide (2) binary system with liquid composition (whole range of composition) at 100.2 (□), 110.07 (◊), 120.05 (Δ), 127.07 (×) and 130.07 K (o) (symbols this work, dashed line: PR EoS). Error bar: 5%.

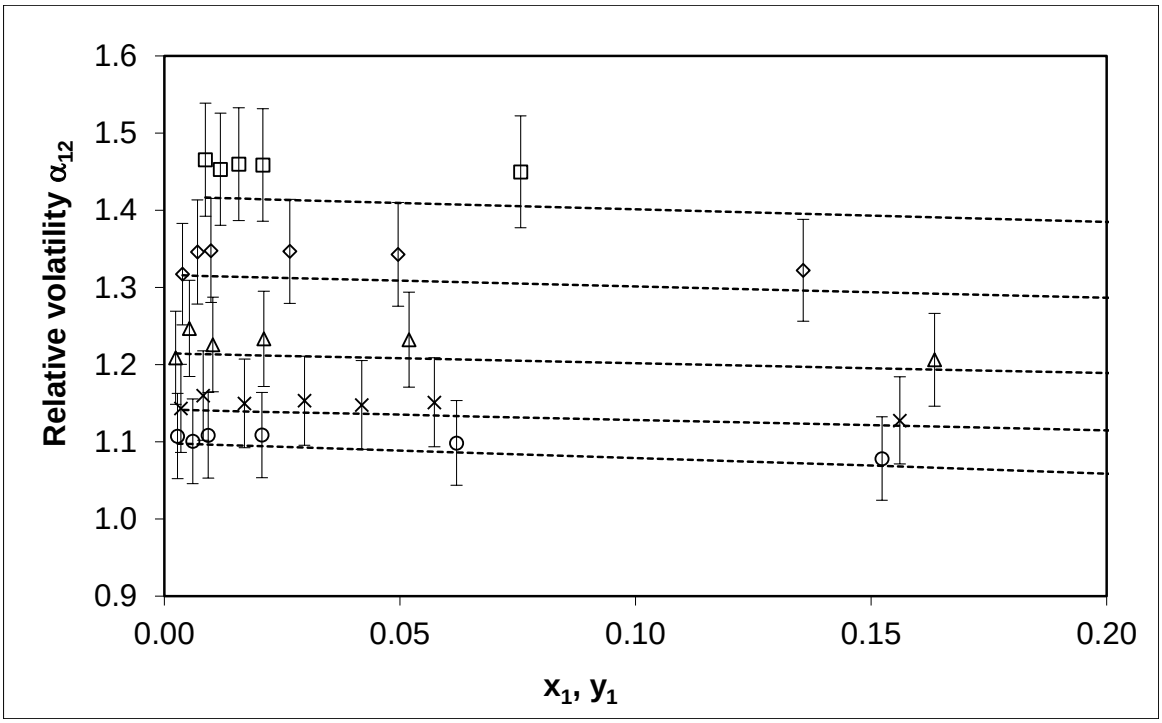

Figure 2b: Variation of the relative volatility α_{12} of the nitrogen (1) + carbon monoxide (2) binary system with liquid composition (between x1=0 and x1=0.2) at 100.2 (□), 110.07 (◊), 120.05 (Δ), 127.07 (×) and 130.07 K (o) (symbols this work, dashed line: PR EoS). Error bar: 5%.

Table 3: Experimental and calculated vapor–liquid equilibrium pressures and phase compositions for the N_2 (1) + CO (2) binary system at the different studied temperatures (δ_{z1} standard deviation of the composition).

Experimental data						Calculated			
T / K	P / MPa	x_1	δx_1	y_1	δy_1	P_{DEW} / MPa	x_1	P_{BUBBLE} / MPa	y_1
100.02 K									
100.01	0.5406	0		0		0.5455	0	0.5455	0
100.01	0.5431	0.0087	0.00001	0.0127	0.00001	0.5480	0.0090	0.5479	0.0123
100.01	0.5441	0.0119	0.00001	0.0172	0.00002	0.5489	0.0122	0.5488	0.0168
100.01	0.5453	0.0158	0.00002	0.0229	0.00002	0.5500	0.0163	0.5498	0.0222
100.02	0.5470	0.0209	0.00001	0.0302	0.00003	0.5518	0.0215	0.5516	0.0293
100.03	0.5639	0.0756	0.00003	0.1060	0.00005	0.5673	0.0778	0.5667	0.1031
100.01	0.6116	0.2512	0.0004	0.3241	0.0002	0.6129	0.2585	0.6111	0.3159
100.01	0.6435	0.3839	0.0007	0.4616	0.0001	0.6445	0.3875	0.6437	0.4579
100.01	0.6695	0.4938	0.002	0.5651	0.0009	0.6694	0.4926	0.6697	0.5663
100.02	0.6954	0.5993	0.0006	0.6653	0.00004	0.6948	0.6006	0.6945	0.6641
100.03	0.7354	0.7834	0.0002	0.8215	0.0002	0.7354	0.7804	0.7361	0.8240
100.04	0.7421	0.8126	0.0003	0.8459	0.0001	0.7423	0.8097	0.7429	0.8483
99.92	0.7762	1		1		0.7763	1	0.7763	1
110.07 K									
110.07	1.0680	0.0000		0.0000		1.0725	0.0000	1.0725	0.0000
110.05	1.0684	0.0038	0.00001	0.0050	0.00001	1.0730	0.0038	1.0730	0.0050
110.06	1.0700	0.0070	0.00001	0.0094	0.00001	1.0752	0.0072	1.0751	0.0092
110.06	1.0718	0.0099	0.00001	0.0133	0.00001	1.0766	0.0101	1.0765	0.0130
110.07	1.0792	0.0266	0.00001	0.0355	0.00005	1.0852	0.0273	1.0849	0.0346
110.06	1.0913	0.0496	0.00001	0.0655	0.00005	1.0954	0.0508	1.0949	0.0639
110.06	1.1323	0.1356	0.0002	0.1718	0.0004	1.1350	0.1380	1.1339	0.1690
110.07	1.1942	0.2702	0.0003	0.3252	0.0001	1.1953	0.2741	1.1937	0.3210
110.07	1.2705	0.4534	0.0002	0.5105	0.0003	1.2710	0.4546	1.2705	0.5093
110.07	1.3297	0.6013	0.0002	0.6491	0.0001	1.3295	0.6003	1.3299	0.6500
110.08	1.4176	0.8240	0.0001	0.8482	0.0001	1.4157	0.8229	1.4161	0.8492
109.91	1.4708	1.0000		1.0000		1.4659	1	1.4659	1
120.05									
120.03	1.8815	0.0000		0.0000		1.8853	0	1.8853	0
120.03	1.8831	0.0024	0.00001	0.0029	0.00001	1.8870	0.0024	1.8870	0.0029
120.04	1.8864	0.0053	0.00001	0.0066	0.00001	1.8902	0.0054	1.8901	0.0064
120.04	1.8907	0.0103	0.00001	0.0126	0.00001	1.8938	0.0104	1.8937	0.0125
120.05	1.8993	0.0211	0.00001	0.0259	0.00001	1.9027	0.0215	1.9025	0.0255
120.04	1.9222	0.0519	0.00006	0.0632	0.00004	1.9242	0.0529	1.9235	0.0620
120.06	2.0014	0.1635	0.0005	0.1908	0.0002	2.0050	0.1650	2.0040	0.1892
120.05	2.1057	0.3112	0.0003	0.3500	0.0009	2.1056	0.3142	2.1036	0.3469
120.05	2.2008	0.4603	0.0002	0.4978	0.0001	2.2023	0.4612	2.2018	0.4969
120.03	2.2558	0.5421	0.0003	0.5792	0.0005	2.2539	0.5451	2.2520	0.5763
120.06	2.2965	0.6047	0.0002	0.6368	0.0006	2.2957	0.6056	2.2951	0.6359
120.06	2.3750	0.7369	0.0001	0.7590	0.0003	2.3767	0.7364	2.3771	0.7595
120.06	2.4417	0.8466	0.0001	0.8603	0.0001	2.4434	0.8466	2.4434	0.8603
119.92	2.5348	1.0000		1.0000		2.5159	1	2.5159	1
127.07									
127.09	2.6717	0.0000		0.0000		2.6804	0	2.6804	0
127.09	2.6755	0.0035	0.00001	0.0040	0.00001	2.6839	0.0035	2.6839	0.0040
127.08	2.6798	0.0082	0.00001	0.0095	0.00001	2.6874	0.0083	2.6872	0.0093

127.09	2.6893	0.0170	0.00002	0.0195	0.00001	2.6973	0.0172	2.6972	0.0193
127.09	2.7024	0.0297	0.00002	0.0341	0.00001	2.7101	0.0301	2.7097	0.0336
127.05	2.7141	0.0419	0.00003	0.0478	0.00002	2.7169	0.0423	2.7165	0.0473
127.09	2.7292	0.0573	0.00002	0.0654	0.00001	2.7375	0.0582	2.7366	0.0644
127.05	2.8254	0.1561	0.0003	0.1726	0.0004	2.8271	0.1572	2.8261	0.1714
127.04	2.9619	0.3002	0.0006	0.3229	0.0001	2.9605	0.3030	2.9580	0.3201
127.06	3.0983	0.4505	0.0014	0.4731	0.0002	3.0982	0.4552	3.0942	0.4686
127.06	3.2045	0.5763	0.0003	0.5926	0.0001	3.2041	0.5792	3.2017	0.5898
					130.07				
130.08	3.0785	0.0000		0.0000		3.0807	0	3.0807	0
130.07	3.0811	0.0028	0.00001	0.0031	0.00001	3.0825	0.0028	3.0824	0.0031
130.07	3.0852	0.0060	0.00001	0.0066	0.00001	3.0860	0.0060	3.0860	0.0066
130.07	3.0890	0.0093	0.00002	0.0103	0.00001	3.0898	0.0094	3.0897	0.0102
130.07	3.1019	0.0207	0.00001	0.0229	0.00002	3.1027	0.0210	3.1024	0.0226
130.08	3.1482	0.0620	0.00002	0.0677	0.00003	3.1503	0.0627	3.1495	0.0670
130.07	3.2471	0.1523	0.0002	0.1623	0.0004	3.2471	0.1535	3.2458	0.1611
130.08	3.3515	0.2471	0.0006	0.2567	0.0001	3.3460	0.2478	3.3453	0.2560

Expanded uncertainties (k=2):
U(T)=0.03 K, U(P)=0.00015 MPa for pressures lower than 1.5 MPa, U(P)=0.0004 MPa for pressures higher than 1.5 MPa
Standard uncertainties: u(z)=0.0035 for z_1 higher than 0.17 and u(z)=0.0018 for z_1 lower than 0.17.

The adjusted binary interaction parameter (BIP) corresponding to the quadratic mixing rules associated to the PR EoS, and the given deviations (AAD and Bias), are specified in the Table 4. The deviations (the ARD and the Bias) applied on pressures and liquid and vapor phase mole fractions, are defined by Eqs. (5-6).

$$ARD\ /\% = \left(\frac{100}{N}\right)\sum_{i=1}^{N}\left|\frac{U_{exp}-U_{cal}}{U_{exp}}\right| \quad (5)$$

$$Bias\ /\% = \left(\frac{100}{N}\right)\sum_{i=1}^{N}\left(\frac{U_{exp}-U_{cal}}{U_{exp}}\right) \quad (6)$$

Where N is the number of data points, and $U = P$, x_1 or y_1.

Table 4: Values of the binary interaction parameter (k_{ij}) and deviations with Peng Robinson EoS for the new experimental data.

T/K	k_{ij}	Bias P/%	ARD P/%	bias x /%	ARD x/%	bias y/%	ARD y/%
			This work				
100.02	0.0063	-0.39	0.42	-1.66	1.84	1.57	1.71
110.07	0.0072	-0.20	0.28	-1.32	1.38	1.26	1.31
120.05	0.0074	-0.03	0.17	-0.80	0.89	0.77	0.86
127.07	0.0101	-0.16	0.19	-1.00	1.00	0.96	0.96
130.07	0.0116	-0.03	0.04	-0.90	0.90	0.88	0.88
			Constant kij value				
127.07	0.01084	-0.2	0.2	-0.89	0.89	0.85	0.85
130.07		-0.02	0.04	-1.0	1.0	0.99	0.99
			Torochesnikov [8]				
70	0.0031	0.44	1.25	-2.09	2.58	1.39	1.82

75	0.0012	0.10	0.58	0.34	1.97	-0.47	1.58
80	0.0216	1.97	2.21	4.14	6.66	-4.12	5.88
85	0.0353	3.55	3.76	6.13	8.80	-5.99	7.95
90	-0.0030	0.35	2.58	1.11	1.95	-0.93	1.71
95	-0.0120	-0.32	1.13	0.13	2.94	-0.10	2.58
100	0.0034	0.69	1.67	1.72	2.27	-1.58	2.09
105	0.0140	0.73	1.25	1.98	2.44	-1.86	2.23
110	0.0012	0.37	1.00	0.81	1.89	-0.77	1.76
115	0.0025	0.49	0.93	0.53	1.44	-0.50	1.34
120	0.0026	0.59	0.99	-0.14	1.01	0.12	0.94
122	-0.0011	0.43	0.66	-0.39	0.82	0.36	0.77
Yushkevich and Toroshechnikov [9]							
70	-0.0030	0.28	1.32	-4.77	4.77	3.26	3.26
75	0.0005	0.26	0.94	0.98	1.44	-0.83	1.13
79.2	0.0059	0.25	1.26	4.60	4.60	-3.86	3.86
90.1	0.0103	2.01	2.52	6.75	6.75	-6.75	6.75
96.7	-0.0100	0.99	1.44	1.12	2.14	-0.95	1.91
100	0.0041	1.78	1.78	8.21	8.21	-8.22	8.22
105.1	0.0146	1.24	1.80	6.89	6.89	-6.71	6.71
110	0.0030	0.56	0.96	2.95	2.95	-2.83	2.83
116.6	0.0029	0.61	0.99	1.21	1.21	-1.13	1.13
121.8	0.0017	1.01	1.11	2.55	2.55	-2.55	2.55
Duncan and Staveley [11]							
68.09	0.0060	-1.84	1.84				
Sprow and Prausnitz [7]							
83.82	0.0060	-0.59	0.69	-1.75	1.96	1.48	1.62
Pool et al. [10]							
83.82	0.0057	-0.36	0.54				

We can observe from Table 4 that our experimental data are well correlated by the model. There are no systematic deviations as absolute values of Bias are different from ARD values, nevertheless we agree that the model tend to slightly overestimate pressure and N2 liquid mole fraction, and slightly underestimate N2 vapor mol fraction, relatively to the raw data. The variation of the BIP with the temperature is plotted on Fig. 3. The BIPs values are relatively low (close to 0) since the both components have very close critical temperature values (the $T_{c, CO}$ is slightly higher due to the polarity of CO). We can see a relative constant value of the BIP for temperatures lower than the critical temperature of nitrogen and a discontinuity of the temperature above the nitrogen critical temperature. This point was already observed by the authors in previous publications Chapoy et al. [18] but also in Valtz et al. [19] and Kato et al. [20]. This discontinuity can be due to the

fact that the lightest component is at its supercritical phase state and not gas phase state leading to a change of the molecular interaction between the two components. Also, approaching the critical temperature of nitrogen, we may have important fluctuation of density which disappear after increasing of temperature as explained by Courtial et al. [21].

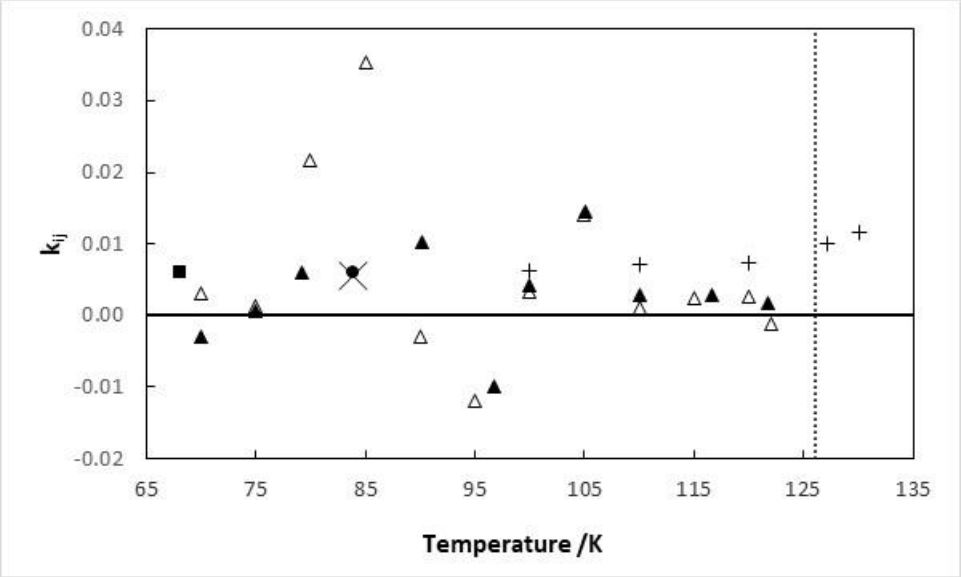

Figure 3: Variation of the binary interaction parameter with the temperature. (■): Duncan and Staveley, (Δ): Torocheshnikov, (●): Sprow and Prausnitz, (▲): Yushkevich and Torocheshnikov, (×): Pool et al., (+): this work. Dotted line: critical temperature of nitrogen.

4.2. Literature data

We have applied the same thermodynamic model to correlate the literature data. The results are presented in Table 4 (binary interaction parameters and deviations). As we can see, the data from Torocheshnikov and Yushkevich and Torocheshnikov are not well represented by our model. There are important deviations on liquid and vapor compositions. As we can see on the Figs. 4a and 4b, with the data from Torocheshnikov, there is problem with the value of the CO pure component vapor pressure.

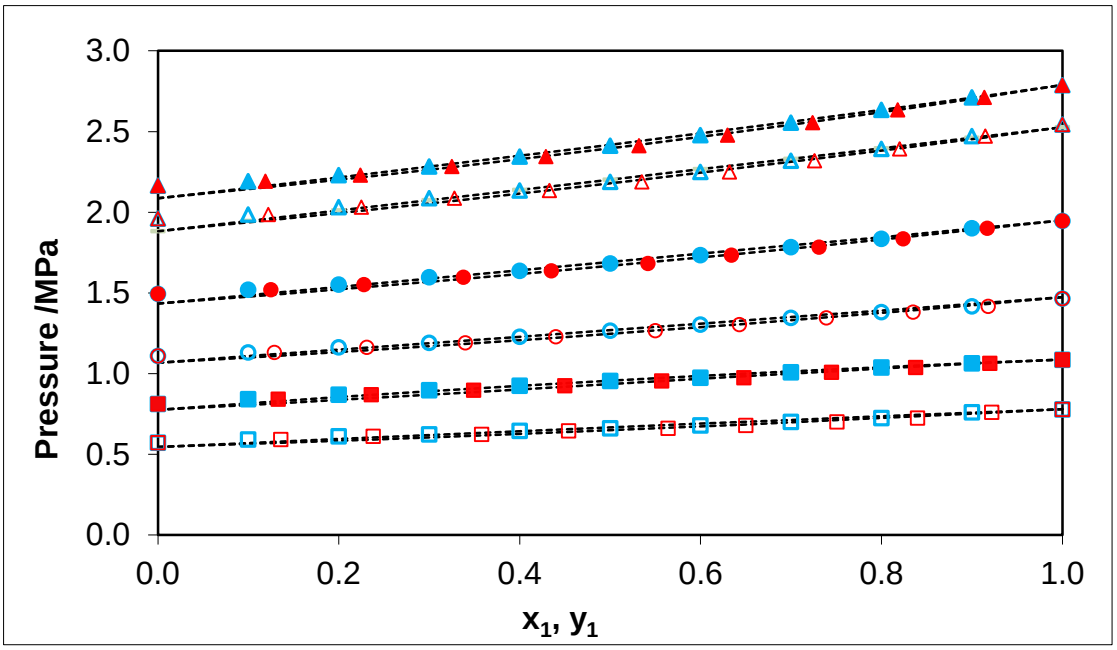

Figure 4a: Vapor liquid Equilibrium data for the nitrogen (1) + carbon monoxide (2) binary system from 100 (□), 105 (■), 110 (o), 115 (●), 120 (Δ) and 122 K (▲), in blue: bubble point, in red: dew point. Experimental data from Torocheshnikov [8]. Dashed line: Peng Robinson EoS.

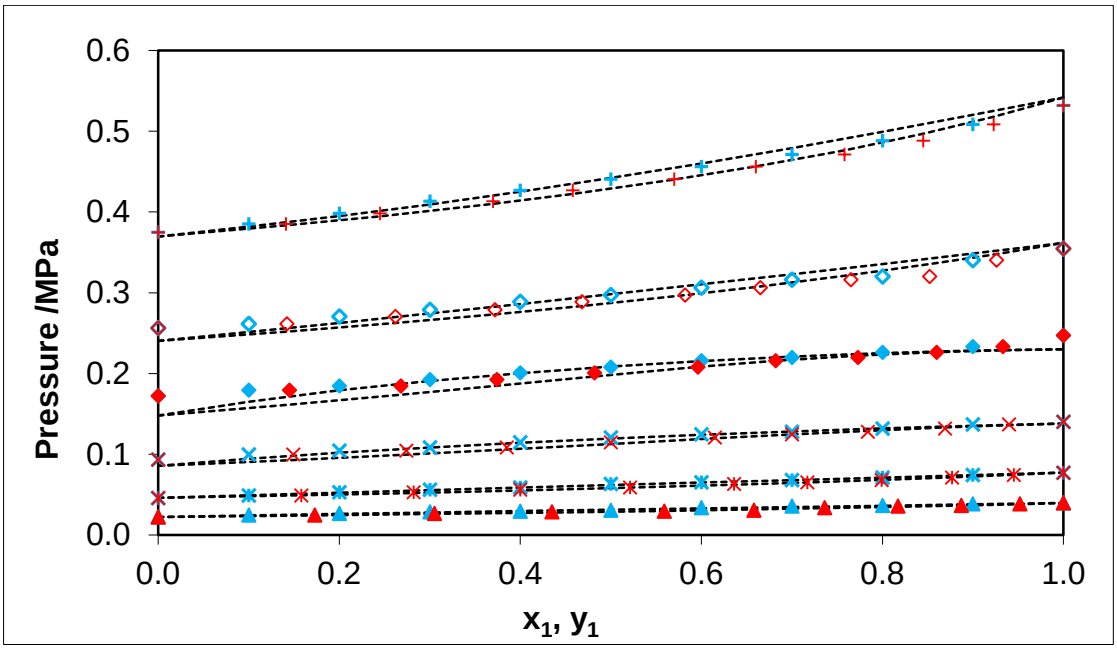

Figure 4b: Vapor liquid Equilibrium data for the nitrogen (1) + carbon monoxide (2) binary system from 70 (▲), 75 (*), 80 (×), 85 (♦), 90 (◊) and 95 K (+), in blue: bubble point, in red: dew point. Experimental data from Torocheshnikov [8]. Dashed line: Peng Robinson EoS.

Furthermore, the ARD found for CO vapor pressure measurements in comparison to the prediction from DIPPR correlation (Eq. 7) [13] is equal to 0.41 % for our data, 5.55 % for Torocheshnikov's data and 5.28 % for Yushkevich and Torochechnikov's data. The value for the data from Sprow and Prausnitz at 83.82 K is equal to 1.07%. The value for the data from Duncan and Staveley at 68.09 K is equal to 0.65%.

$$P\ /Pa = e^{A+\frac{B}{T}+Cln(T)+DT^{E}} \quad (7)$$

With A=45.698, B=-1076.6, C=-4.8814, D=7.5763×10^{-5} and E=2. These parameters were taken from Simulis thermodynamics (PROSIM, France).

Comparisons between the prediction from DIPPR's correlation and experimental data are presented in the Fig. 5. Probably there is a problem with the quality of the pure carbon monoxide used by Torocheshnikov and Yushkevich and Torochechnikov. This is the main reason which explain why their data are not well represented by the model.

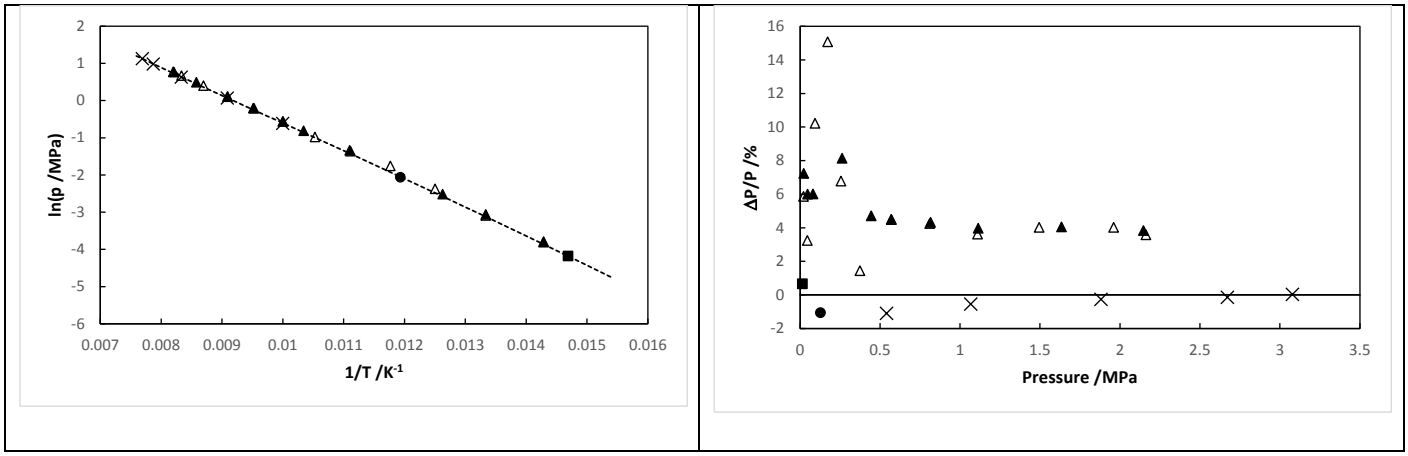

Figure 5. A: Vapor pressure of carbon monoxide as a function of temperature, experimental and calculated values (solid line: prediction from DIPPR's correlation (■): Duncan and Staveley, (Δ): Torocheshnikov, (●): Sprow and Prausnitz, (▲): Yushkevich and Torocheshnikov, (×): this work.). B: Relative deviations of CO vapor pressure from the different authors in comparison to the DIPPR correlation's prediction.

4.3. Comparison with Gernet and Span's model predictons

As Gernet and Span have used the vapor liquid equilibrium literature data cited in this work to adjust the binary interaction parameters of their Helmholtz energy mixture model, we have compared the prediction of their model available in REFPROP 10.0 [22] software with our experimental data. The results are presented in Table 5 and plotted on Fig. 6. Despite the potentially superior qualities of the GERG 2008 equation of state compared to the Peng-Robinson equation of state, as we can see, the deviations are very important because the parameters were adjusted using literature VLE data with very limited quality and range of composition as explained above. It is necessary to consider our new set of data in the adjustment of the Helmholtz energy mixture model and particularly the data measurement for temperature higher than the critical temperature of nitrogen.

Table 5: Values deviations with the Helmholtz energy mixture model for the new experimental data.

T/K	Bias P/%	ARD P/%	bias x /%	ARD x/%	bias y/%	ARD y/%
100.02	0.16	0.82	20.3	20.3	1.55	1.71
110.07	0.31	0.55	17.8	17.8	1.56	1.67
120.05	0.54	0.54	11.45	11.45	0.73	0.84
127.07	0.41	0.41	9.54	9.54	0.78	0.81
130.07	0.33	0.33	7.85	7.85	0.52	0.58

Also, we have compared the values of mixture critical point using the PR EoS and the Helmholtz energy mixture model parametrized by Gernet and Span. To compute the mixture critical point line using the PR EOS we have considered a binary interaction parameter with a constant value in order to avoid bad prediction due to the temperature dependency of the BIP. This BIP is adjusted on isotherm for temperature higher than the critical temperature of nitrogen, deviations are presented in Table 4. Results are reported in Table 6 and plotted in Fig. 1 (for the mixture critical point line) and Fig 6. It seems that the model developed by Gernet and Span predicts higher critical pressure values than the

ones predict by the Peng Robinson EoS. Moreover, the Fig. 6 seems to confirm a type I behavior according to the classification of van Konynenburg and Scott for the nitrogen + carbon monoxide binary system.

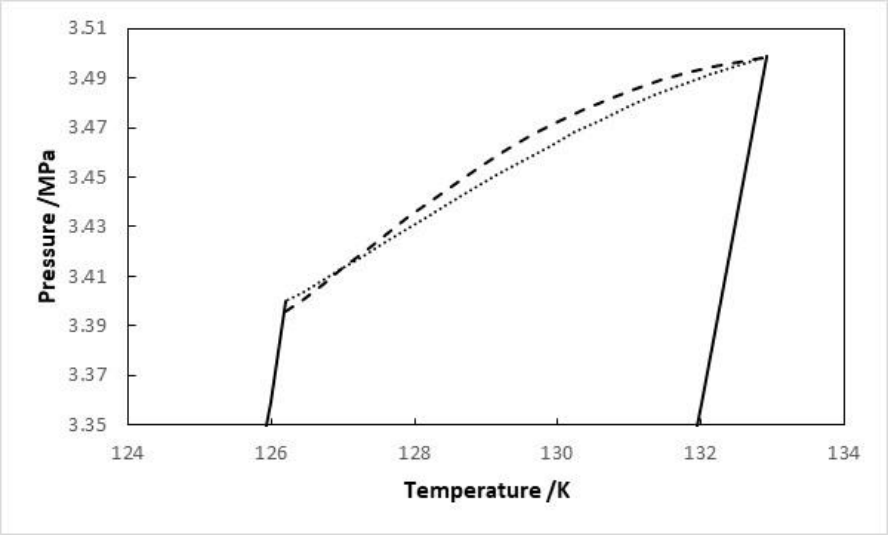

Figure 6: Comparison between the nitrogen + carbon monoxide mixture critical point predicted by Gernet and Span model (dotted line) and Peng Robinson Equation of state with binary interaction parameters adjusted on our experimental data (constant value k_{ij}=0.01084) (dashed line). Solid line: the two pure component vapor pressures.

Table 6: Predicted nitrogen (1) + carbon monoxide (2) mixture critical point values by the Peng Robinson Equation of state with binary interaction parameters adjusted on the new experimental data (constant value k_{ij}=0.01084) and by Gernet and Span model.

Composition	PR EoS		Gernet and Span model	
z_1	T_C /K	P_C /MPa	T_C /K	P_C /MPa
0	132.92	3.499	132.86	3.498
0.05	132.52	3.495	132.51	3.496
0.1	132.12	3.492	132.15	3.494
0.15	131.73	3.488	131.79	3.492
0.2	131.35	3.483	131.44	3.489
0.25	130.97	3.478	131.08	3.486
0.3	130.60	3.473	130.71	3.482
0.35	130.23	3.468	130.35	3.477
0.4	129.87	3.463	129.99	3.472
0.45	129.52	3.457	129.64	3.467
0.5	129.17	3.451	129.28	3.461
0.55	128.83	3.446	128.93	3.455
0.6	128.50	3.440	128.59	3.448
0.65	128.18	3.434	128.25	3.441
0.7	127.87	3.429	127.92	3.434
0.75	127.57	3.423	127.60	3.427
0.8	127.27	3.418	127.29	3.420
0.85	126.99	3.413	126.99	3.413
0.9	126.71	3.408	126.71	3.407
0.95	126.45	3.404	126.44	3.401
1	126.20	3.400	126.19	3.396

5. Conclusion.

In this paper we present VLE data for the system N_2 (1) + CO (2) at 5 temperatures, 3 temperatures below and 2 temperatures above the nitrogen critical temperature. We have used an equipment whom experimental technique is based on the "static-analytic" method to obtain the experimental data. The Peng-Robinson EoS was considered to adjust the binary interaction parameters on the new experimental data. The experimental results were compared to literature data and we have concluded that some literature data were suspicious because deviations were very important on pressure but almost on vapor and liquid compositions. Moreover, the new experimental results describe successfully the N_2 (1) + CO (2) binary system especially for low nitrogen content as it could be expected to design distillation column for CO purification purpose.

Acknowledgment

The authors want to thanks the Air Liquide Company for its financial support.

Supplementary Material

Supplementary figures of phase diagrams
Checking the thermodynamic consistency of the VLE data using a Van Ness type test.

List of symbols:

a	Parameter of the equation of state (energy parameter [J. m^3.mol^{-2}])
b	Parameter of the equation of state (molar co volume parameter [m^3.mol^{-1}])
A	GC peak surface area
F	Objective function
K_{ij}	Equilibrium coefficient
k_{ij}	Binary interaction parameter
N	Number of data points
P	Pressure [Pa or MPa]
R	Gas constant [J.mol^{-1}.K^{-1}]
T	Temperature [K]
x	Liquid mole fraction
U	P, *x or y*
y	Vapor mole fraction
α_{ij}	Relative volatility

Superscript

E	Excess property

Subscripts

C	Critical property
cal	Calculated property
exp	Experimental property
i,j	Molecular species
1	Nitrogen (N_2)
2	Carbon monoxide (CO)

References:

[1] C. Coquelet, P. Stringari, M. Hajiw, A. Gonzalez, L. Pereira, M. Nazeri, R. Burgass, A. Chapoy, Transport of CO2: presentation of new thermophysical property measurements and phase diagrams, Energy Procedia, 114 (2017) 6844-6859.
[2] C. Coquelet, A. Valtz, F. Dieu, D. Richon, P. Arpentinier, F. Lockwood, Isothermal P, x, y data for the argon+ carbon dioxide system at six temperatures from 233.32 to 299.21 K and pressures up to 14 MPa, Fluid Phase Equilib., 273 (2008) 38-43.
[3] C. Coquelet, A. Valtz, P. Arpentinier, Thermodynamic study of binary and ternary systems containing CO2+ impurities in the context of CO2 transportation, Fluid Phase Equilib., 382 (2014) 205-211.
[4] F. Zhang, E. El Ahmar, A. Valtz, E. Boonaert, C. Coquelet, A. Chapoy, Phase Equilibrium of Three Binary Mixtures Containing NO and Components Present in Ambient Air, J. Chem. Eng. Data, 63 (2018) 1021-1026.
[5] P. Van Konynenburg, R. Scott, Critical lines and phase equilibria in binary van der Waals mixtures, Phil. Trans. R. Soc. Lond. A, 298 (1980) 495-540.
[6] J. Gernert, R. Span, EOS–CG: A Helmholtz energy mixture model for humid gases and CCS mixtures, The Journal of Chemical Thermodynamics, 93 (2016) 274-293.
[7] F. Sprow, J. Prausnitz, Vapor- Liquid equilibria for five cryogenic mixtures, AIChE Journal, 12 (1966) 780-784.
[8] N. Torocheshnikov, Isotherms and isobars of the nitrogen-carbon monoxide system, Tech. Phys. USSR, 4 (1937) 365-369.
[9] N. Yushkevich, N. Torocheshaikov, The coexistence of liquid and vapor phases in solutions of nitrogen and carbon monoxide, J. CHEM. IND.(USSR), 13 (1936) 1273-1283.
[10] R. Pool, G. Saville, T. Herrington, B. Shields, L. Staveley, Some excess thermodynamic functions for the liquid systems argon+ oxygen, argon+ nitrogen, nitrogen+ oxygen, nitrogen+ carbon monoxide, and argon+ carbon monoxide, Trans. Faraday Society, 58 (1962) 1692-1704.
[11] A. Duncan, L. Staveley, Thermodynamic functions for the liquid systems argon+ carbon monoxide, oxygen+ nitrogen, and carbon monoxide+ nitrogen, Trans. Faraday Society, 62 (1966) 548-552.
[12] D. Houssin-Agbomson, C. Coquelet, D. Richon, P. Arpentinier, Equipment using a "static-analytic" method for solubility measurements in potentially hazardous binary mixtures under cryogenic temperatures, Cryogenics, 50 (2010) 248-256.
[13] R.C. Reid, J.M. Prausnitz, B.E. Poling, The properties of gases and liquids, (1987).
[14] A. Muhlbauer, Phase Equilibria: Measurement & Computation, CRC press, 1997.
[15] ALLPROPS-Property Package (version 6). Center for Applied Thermodynamic Studies. , in, University of Idaho (Moscow), 1996.
[16] P. Guilbot, A. Valtz, H. Legendre, D. Richon, Rapid on-line sampler-injector: a reliable tool for HT-HP sampling and on-line GC analysis, Analusis, 28 (2000) 426-431.
[17] D.-Y. Peng, D.B. Robinson, A new two-constant equation of state, Ind. Eng. Chem. Fundam., 15 (1976) 59-64.
[18] A. Chapoy, M. Nazeri, M. Kapateh, R. Burgass, C. Coquelet, B. Tohidi, Effect of impurities on thermophysical properties and phase behaviour of a CO2-rich system in CCS, Int. J. Greenhouse Gas Control, 19 (2013) 92-100.

[19] A. Valtz, C. Coquelet, A. Baba-Ahmed, D. Richon, Vapor–liquid equilibrium data for the CO2+ 1, 1, 1, 2, 3, 3, 3,-heptafluoropropane (R227ea) system at temperatures from 276.01 to 367.30 K and pressures up to 7.4 MPa, Fluid Phase Equilib., 207 (2003) 53-67.
[20] M. Kato, W. Chung, B.C.-Y. Lu, Binary interaction coefficients of the Redlich—Kwong equation of state, Chem. Eng. Sci., 31 (1976) 733-736.

[21] X. Courtial, C.B. Soo, C. Coquelet, P. Paricaud, D. Ramjugernath, D. Richon, Vapor Liquid equilibrium in the n-butane + methanol system, measurement and modeling from 323.2 to 443.2 K, Fluid Phase Equilib., 277 (2009) 152-161.

[22] E. Lemmon, I.H. Bell, M. Huber, M. McLinden, NIST Standard Reference Database 23: Reference Fluid Thermodynamic and Transport Properties-REFPROP, Version 10.0, National Institute of Standards and Technology, (2018).